Critical Velocity and Dissipation of an Ultracold Bose-Fermi Counterflow

Marion Delehaye, Sébastien Laurent, Igor Ferrier-Barbut,* Shuwei Jin, Frédéric Chevy, and Christophe Salomon
Laboratoire Kastler Brossel, ENS-PSL, CNRS, UPMC-Sorbonne Universités, and Collège de France, 75005 Paris, France
(Received 10 October 2015; revised manuscript received 19 November 2015; published 23 December 2015)

We study the dynamics of counterflowing bosonic and fermionic lithium atoms. First, by tuning the interaction strength we measure the critical velocity v_c of the system in the BEC-BCS crossover in the low temperature regime and we compare it to the recent prediction of Castin *et al.*, C. R. Phys. 16, 241 (2015). Second, raising the temperature of the mixture slightly above the superfluid transitions reveals an unexpected phase locking of the oscillations of the clouds induced by dissipation.

DOI: 10.1103/PhysRevLett.115.265303 PACS numbers: 67.85.-d, 03.75.Kk, 03.75.Ss, 37.10.Gh

Superconductivity and superfluidity are spectacular macroscopic manifestations of quantum physics at low temperature. Besides liquid helium 4 and helium 3, dilute quantum gases have emerged over the years as a versatile tool to probe superfluid properties in diverse and controlled situations. Frictionless flows have been observed with both bosonic and fermionic atomic species, in different geometries and in a large range of interaction parameters from the weakly interacting Bose gas to strongly correlated fermionic systems [1–6]. Several other hallmarks of superfluidity such as quantized vortices or second sound were also observed in cold atoms [7–9].

A peculiar feature of superfluid flows is the existence of a critical velocity above which dissipation arises. In Landau's original argument, this velocity is associated with the threshold for creation of elementary excitations in the superfluid: for a linear dispersion relation, it predicts that the critical velocity is simply given by the sound velocity in the quantum liquid. This critical velocity has been measured both in superfluid helium [10] and ultracold atoms [1,4–6,11]. However, the recent production of a Bose-Fermi double superfluid [12] raised new questions on Bose-Fermi mixtures [13–16] and interrogations on the validity of Landau's argument in the case of superfluid counterflow [17–22].

In this Letter, we study the dynamics of a Bose-Fermi superfluid counterflow in the crossover between the Bose-Einstein condensate (BEC) and Bardeen-Cooper-Schrieffer (BCS) regimes and at finite temperature. We show how friction arises when the relative velocity of the Bose and Fermi clouds increases and we confirm that damping occurs only above a certain critical relative velocity v_c. We compare our measurements to Landau's prediction and its recent generalization $v_c = c_s^F + c_s^B$, where c_s^F and c_s^B are the sound velocities of the fermionic and bosonic components, respectively [18]. Finally, we study finite temperature damping of the counterflow and we show that the system can be mapped onto a Caldeira-Leggett-like model [23] of two quantum harmonic oscillators coupled to a bath of excitations. This problem has been recently studied as a toy model for decoherence in quantum networks [24] or for heat transport in crystals [25] and we show here that the emergence of dissipation between the two clouds leads to a Zeno-like effect which locks their relative motions.

Our Bose and Fermi double-superfluid setup was previously described in [12]. We prepare vapors of bosonic (B) ^{7}Li atoms spin polarized in the second-to-lowest energy state and fermionic (F) ^{6}Li atoms prepared in a balanced mixture of the two lowest spin states noted $|\uparrow\rangle$, $|\downarrow\rangle$. The two species are kept in the same cigar-shaped hybrid magnetic-optical trap in which evaporative cooling is performed in the vicinity of the 832 G ^{6}Li Feshbach resonance [26]. The final number of fermions $N_F = 2.5 \times 10^5$ greatly exceeds that of the bosons $N_B \sim 2.5 \times 10^4$ and the temperature of the sample is adjusted by stopping the evaporation at different trap depths. The thermal pedestal surrounding the ^{7}Li BEC provides a convenient low temperature thermometer for both species after sufficiently long thermalization time (~1 sec). The lowest temperature achieved in this study corresponds to almost entirely superfluid clouds with $T/T_{c,\alpha=B,F} \leq 0.5$, where $T_{c,\alpha}$ is the superfluidity transition temperature of species α.

The magnetic field values used in the experiment (780–880 G) enable us to scan the fermion-fermion interaction within a range $-0.5 \leq 1/k_F a_F \leq 1$. Here, a_F is the s-wave scattering length between $|\uparrow\rangle$ and $|\downarrow\rangle$ fermions and the Fermi momentum k_F is defined by $\hbar^2 k_F^2/2m_F = \hbar\bar{\omega}(3N_F)^{1/3}$ with $\bar{\omega}$ the geometric mean of the trap frequencies, and N_F the total number of fermions of mass m_F. In our shallowest traps, typical trap frequencies for ^{6}Li are $\omega_x = \omega_y = 2\pi \times 550$ Hz and $\omega_z = 2\pi \times 17$ Hz. Since the bosonic and fermionic isotopes experience the same trapping potentials, the oscillation frequencies of the two species are within a ratio $\sqrt{6/7} \simeq 0.9$.

We excite the dipole modes of the system by displacing adiabatically the centers of mass of the clouds from their initial position by a distance z_0 along the weakly confined z direction, and abruptly releasing them in the trap. The two clouds evolve for a variable time t before *in situ* absorption images perpendicular to the z direction are taken. The measurement of their doubly integrated density profiles gives access to axial positions and atom numbers of both species. Typical time evolutions of the centers of mass are shown in Fig. 1 for different parameter values. Since the Bose and Fermi components oscillate at different frequencies, they oscillate in quadrature after a few periods. By changing z_0, we can thus tune the maximum relative velocity between the two clouds and probe the critical superfluid counterflow.

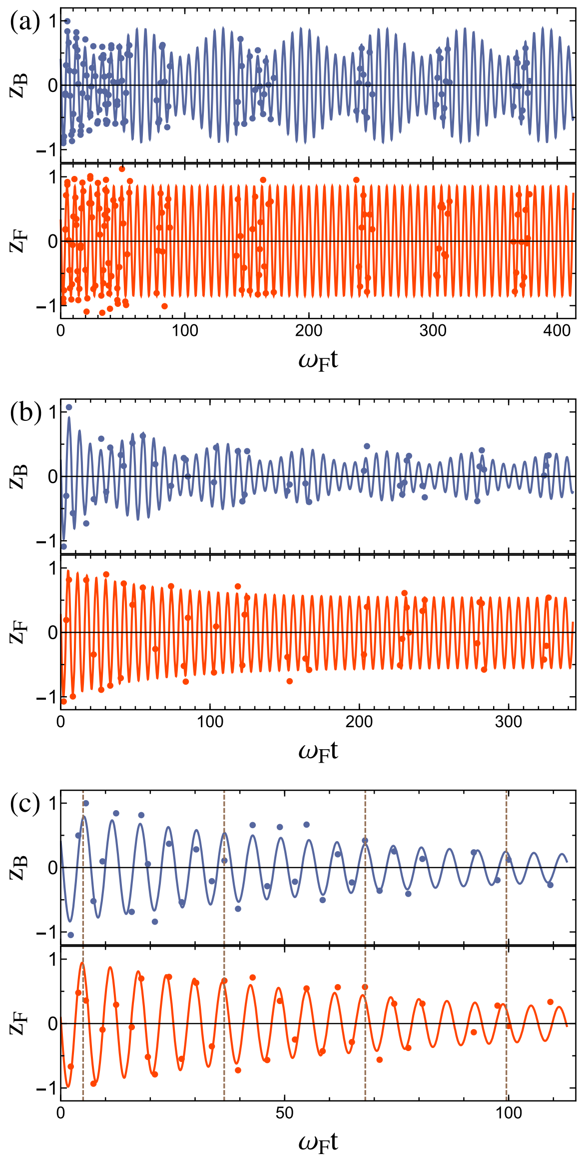

FIG. 1 (color online). Center-of-mass oscillations of bosons (blue, top) and fermions (red, bottom), for different sets of parameters at unitarity. Solid lines: fits using Eq. (1) for the bosons and a similar equation for the fermions. (a) $T/T_F = 0.03$, $T/T_{c,b} \leq 0.5$, $z_0 = 10\ \mu$m. Superfluid regime, no damping is observed and $\omega_B = 2\pi \times 15.41(1)$ Hz $\approx \sqrt{6/7}\omega_F$. The observed beating at $\omega_F - \omega_B$ is due to coherent energy exchange between the clouds. (b) $T/T_F = 0.03$ and $z_0 = 150\ \mu$m. For a larger initial displacement, initial damping ($\gamma_B = 2.4\ \mathrm{s}^{-1}$) is followed by steady-state evolution. $\omega_B = 2\pi \times 14.2(1)$ Hz $\approx \sqrt{6/7}\omega_F$. (c) $T/T_F = 0.4$ and $z_0 = 80\ \mu$m. At higher temperature, phase locking of the two frequencies is observed with $\omega_F \approx \omega_B = 2\pi \times 17.9(3)$ Hz and $\gamma_B = \gamma_F = 1.4(5)\ \mathrm{s}^{-1}$.

As shown in Fig. 1(a), the superfluid counterflow exhibits no visible damping on a $\simeq 5$ s time scale for very low temperature and small initial displacement. A striking feature is the beat note on the ^{7}Li oscillation amplitude due to the coherent mean-field coupling to the ^{6}Li cloud [12]. For larger relative velocities, ^{7}Li oscillations are initially damped [Fig. 1(b)] until a steady-state regime as in Fig. 1(a) is reached. We fit the time evolution of the cloud position using the phenomenological law

$$z_B(t) = d(t)[a\cos(\omega_B t) + b\cos(\omega_F t)],$$
$$d(t) = d_1 + d_2 \exp(-\gamma_B t). \tag{1}$$

We measure the damping rate γ_B as a function of relative velocity for six different values of magnetic field, exploring a large region of the crossover going from the BCS ($1/k_F a_F = -0.42$, $B = 880$ G) to the BEC side ($1/k_F a_F = 0.68$, $B = 780$ G), see Fig. 2. For these magnetic field values, the Bose gas remains in the weakly interacting (repulsive) regime and the Bose-Fermi scattering length is $a_{BF} \simeq 41 a_0$, constant in this magnetic field range, and equal for both $|\uparrow\rangle$ and $|\downarrow\rangle$ spin states.

We extract the critical velocity v_c using an *ad hoc* power-law fitting function $\gamma_B = A\Theta(v - v_c)[(v - v_c)/v_F]^\alpha$, where Θ is the Heaviside function and v_F is the Fermi velocity given by $v_F = \hbar k_F/m_F$. For details, see [27]. v_c in the BEC-BCS crossover is displayed in Fig. 3 (red dots) and compared to the predictions of Landau and Castin *et al.* [18]. In this latter work, dissipation arises by the creation of excitation pairs and yields a critical velocity

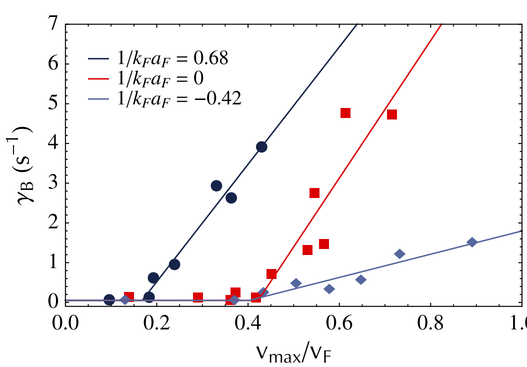

FIG. 2 (color online). Damping rate of the center-of-mass oscillations versus maximal relative velocity in the BEC-BCS crossover in units of the Fermi velocity v_F. Dark blue dots, BEC side (780 G) $1/k_F a_F = 0.68$; red squares, unitarity (832.2 G) $1/k_F a_F = 0$; light blue diamonds, BCS side (880 G) $1/k_F a_F = -0.42$. Power law fits with thresholds provide the critical velocity (solid lines).

$v_c = \mathrm{Min}_{p, \sigma=f,b}\{[\epsilon^B(\boldsymbol{p}) + \epsilon^F_\sigma(\boldsymbol{p})]/[p]\}$. In this expression, $\epsilon^B(\boldsymbol{p})$ denotes the dispersion relation of excitations in the BEC and $\epsilon^F_\sigma(\boldsymbol{p})$ refers to the two possible branches of the Fermi superfluid, phononlike ($\sigma = b$), and threshold for pair breaking excitations ($\sigma = f$) [28]. For homogeneous gases, at unitarity and on the BEC side of the crossover, this critical relative velocity turns out to be simply the sum of the respective sound velocities of the Bose and Fermi superfluids, $v_c = c_s^F + c_s^B$. We thus plot in Fig. 3 the calculated sound velocities of both superfluids in an elongated geometry obtained by integration over the transverse direction [29–33] (red dashed line c_s^F, blue bars c_s^B). Typically, c_s^B contributes ≃20%–25% to the sum shown as green squares in Fig. 3. Around unitarity and on the BCS side of the resonance, our experimental data are consistent with this interpretation as well as with a critical velocity $v_c = c_s^F$ that one would expect by considering the BEC as a single impurity moving inside the fermionic superfluid. By contrast, we clearly exclude the bosonic sound velocity as a threshold for dissipation.

Our measured critical velocities are significantly higher than those previously reported in pure fermionic systems which, for all interaction strengths, were lower than Landau's criterion [4,6]. The main difference with our study is the use of focused laser beams instead of a BEC as a moving obstacle. In [6], the laser beam is piercing the whole cloud including its nonsuperfluid part where the density is low, and its potential may create a strong density modulation of the superfluid. These effects make a direct

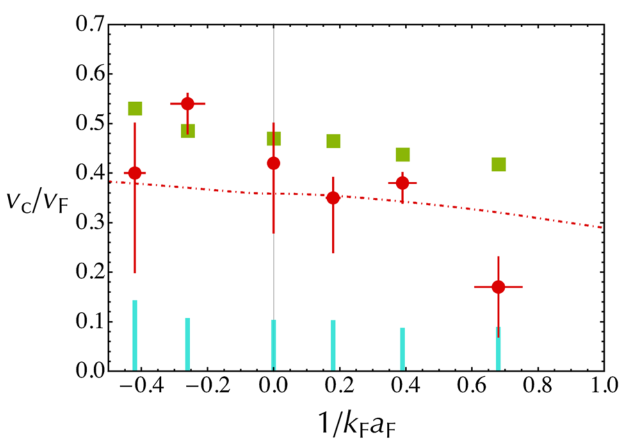

FIG. 3 (color online). Critical velocity of the Bose-Fermi superfluid counterflow in the BEC-BCS crossover normalized to the Fermi velocity v_F. Red dots, measurements. Red dot-dashed line, sound velocity c_s^F of an elongated homogeneous Fermi superfluid calculated from its equation of state [29,30] after integration of the density in the transverse plane, and also measured in [34]. Blue bars, calculated sound velocity c_s^B of the elongated ^{7}Li BEC for each magnetic field (880, 860, 832, 816, 800, 780 G). Green squares indicate the prediction $v_c = c_s^F + c_s^B$. Error bars and c_s^B are discussed in [27].

comparison to Landau criterion difficult [35]. On the contrary, in our system the size of the BEC (Thomas Fermi radii of 73, 3, 3 μm) is much smaller than the typical size of the Fermi cloud (350, 13, 13 μm around unitarity). For oscillation amplitudes up to ±200 μm the BEC probes only the superfluid core of the fermionic cloud. During its oscillatory motion along z the Bose gas may explore the edges of the Fermi superfluid where the density is smaller. However, it is easy to check that the ratio v/c_s^F is maximum when the centers of the two clouds coincide [27]. Finally, as the mean-field interaction between the two clouds is very small [27] our BEC acts as a weakly interacting local probe of the Fermi superfluid.

On the BEC side of the resonance (780 G), however, we observe a strong reduction of the measured critical velocity compared to the predicted values. The effect is strikingly seen in Fig. 2, dark blue dots (see also Supplemental Material [27]). This anomalously small value for positive scattering lengths is consistent with previous measurements [4,6]. Its origin is still unclear but several explanations can be put forward [35]. First, it is well known that vortex shedding can strongly reduce superfluid critical velocity. However, this mechanism requires a strong perturbation. The density of the Bose gas and the mean-field interaction between the two clouds are probably too small for vortex generation through a collective nucleation process. Second, inelastic losses increase on the BEC side of a fermionic Feshbach resonance and heat up the system [36]. This hypothesis is supported by the presence of a clearly visible pedestal in the density profiles of the BEC taken at 780 G. At this value of the magnetic field, we measure a ≃60% condensed fraction, corresponding to a temperature $T/T_{c,B} \simeq 0.5$. Even though the two clouds are still superfluids as demonstrated by the critical behavior around v_c, the increased temperature could be responsible for the decrease of v_c.

We now present results of experiments performed at a higher temperature ($0.03 \lesssim T/T_F \lesssim 0.5$) for $B = 835$ G. For low temperatures ($T/T_F \leq 0.2$), the two clouds remain weakly coupled and, as observed in Fig. 4, the bosonic and fermionic components oscillate at frequencies in the expected ratio $\simeq 0.9 \simeq \sqrt{6/7}$. A new feature emerges for $T \gtrsim T_{c,B} \approx 0.34 T_F > T_{c,F}$ where both gases are in the normal phase. In this "high" temperature regime, the two clouds are locked in phase: ^{7}Li oscillates at ^{6}Li frequency (Fig. 4) and the two components are equally damped [Fig. 1(c)]. This remarkable behavior can be understood as a Zeno effect arising from the increased dissipation between the two components. Indeed, the system can be described as a set of two harmonic oscillators describing, respectively, the macroscopic motion of the global center of mass of the system (Kohn's mode [37]) and the relative motion of the two clouds [27]. These two degrees of freedom are themselves coupled to the "bath" of

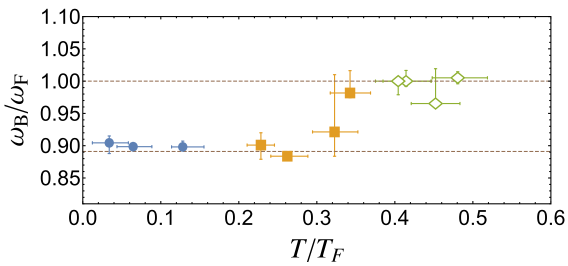

FIG. 4 (color online). Ratio ω_B/ω_F versus temperature of the cloud. Blue circles, the two clouds are superfluids. Yellow squares, only the bosonic component is superfluid. Green open diamonds, the two components are normal. Above $T \approx T_{c,B} \approx 0.34 T_F > T_{c,F}$, oscillations of the Bose and Fermi clouds become locked together at ω_F. Oscillations frequencies are obtained using a Lomb-Scargle algorithm [27]. The lower dashed line is the prediction of a low temperature mean field model [12].

the internal excitations of the two clouds (breathing mode, quadrupole modes, pair breaking excitations…).

In the spirit of the dressed-atom picture, we can represent the state of the two harmonic oscillators by the "radiative" cascade of Fig. 5. Here the states $|N, n\rangle$ are labeled by the quantum numbers associated to Kohn's mode (N) and relative motion (n) of the two clouds and we trace out the degrees of freedom of the bath. On the one hand, Kohn's mode is not an eigenstate of the system for fermions and bosons of different masses; center-of-mass and relative-motion modes are coupled and this coherent coupling is responsible for the dephasing of the oscillations of the two clouds in the weakly interacting regime. On the other hand, interspecies interactions do not act on the center of mass of the whole system, owing to Kohn's theorem, but on the contrary lead to an irreversible "radiative" decay of the *relative* motion at a rate γ.

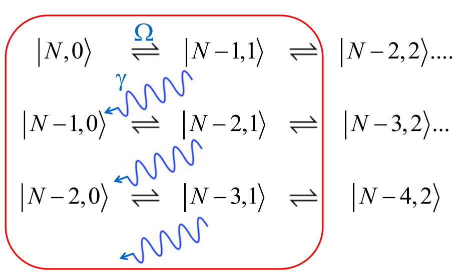

FIG. 5 (color online). Radiative cascade of the center-of-mass motion. In $|N, n\rangle$, N (respectively, n) refers to the center-of-mass (respectively, relative) motion of the two clouds (see text). When the decay rate of the relative motion is larger than the oscillation frequency difference between the two species, the dynamics is restricted to the center-of-mass degree of freedom: in this Zeno-like process, dissipation prevents excitation of the relative motion and the center-of-mass modes of the Bose and Fermi gases do not dephase.

In our experiments, the initial state is a pure center-of-mass excitation $|N, 0\rangle$. If we neglect the interspecies coupling, the system evolves in the subspace spanned by $|N - n, n\rangle_{n=0,\ldots,N}$ of the two coupled oscillators and the system oscillates at a frequency $\delta\omega \simeq \omega_B - \omega_F$ as the centers of mass of the Bose and Fermi clouds dephase. If we now consider the opposite limit where the decay rate γ is larger than the dephasing frequency $\delta\omega$, the strong coupling to the bath prevents the conversion of the center-of-mass excitations into relative motion. As soon as the system is transferred into $|N - 1, 1\rangle$ it decays towards state $|N - 1, 0\rangle$. Similarly to optical pumping in quantum optics, we can eliminate adiabatically the excited states of the relative motion and restrict the dynamics of the system to the subspace $|N, 0\rangle_{N=0,\ldots,\infty}$ of Kohn's excitations. This situation is reminiscent of the synchronization of two spins immersed in a thermal bath predicted in [38] or to phenomenological classical two-coupled oscillators model.

In this Letter, we have investigated how a Bose-Fermi superfluid flow is destabilized by temperature or relative velocity between the two clouds. In the limit of very low temperature the measured critical velocity for superfluid counterflow slightly exceeds the speed of sound of the elongated Fermi superfluid and decreases sharply towards the BEC side of the BEC-BCS crossover. In a future study, we will investigate the role of temperature, of the confining potential, and of the accelerated motion of the two clouds [35] that should provide a more accurate model for the damping rate versus velocity and more insights on the nature of the excitations. In particular, the *ab initio* calculation of the damping rate will require clarification of the dissipation mechanism at play in a trapped system where the bandwidth of the excitation spectrum is narrow, in contrast to a genuine Caldeira-Leggett model [39].

The authors acknowledge support from Institut Francilien de Recherche sur les Atomes Froids (Atomix Project), ERC (ThermoDynaMix Project), and Institut de France (Louis D. Prize). They thank I. Danaila, N. Proukakis, K. L. Lee, and M. Pierce for insightful comments and discussions, and J. Dalibard, Y. Castin, S. Nascimbène, and T. Yefsah for critical reading of the manuscript.

M. D. and S. L. contributed equally to this work.

*Present Address: 5. Physikalisches Institut and Center for Integrated Quantum Science and Technology, Universität Stuttgart, Pfaffenwaldring 57, 70550 Stuttgart, Germany.

[1] C. Raman, M. Köhl, R. Onofrio, D. S. Durfee, C. E. Kuklewicz, Z. Hadzibabic, and W. Ketterle, Phys. Rev. Lett. **83**, 2502 (1999).

[2] A. P. Chikkatur, A. Görlitz, D. M. Stamper-Kurn, S. Inouye, S. Gupta, and W. Ketterle, Phys. Rev. Lett. **85**, 483 (2000).

[3] C. Ryu, M. F. Andersen, P. Cladé, V. Natarajan, K. Helmerson, and W. D. Phillips, Phys. Rev. Lett. **99**, 260401 (2007).
[4] D. E. Miller, J. K. Chin, C. A. Stan, Y. Liu, W. Setiawan, C. Sanner, and W. Ketterle, Phys. Rev. Lett. **99**, 070402 (2007).
[5] R. Desbuquois, L. Chomaz, T. Yefsah, J. Léonard, J. Beugnon, C. Weitenberg, and J. Dalibard, Nat. Phys. **8**, 645 (2012).
[6] W. Weimer, K. Morgener, V. P. Singh, J. Siegl, K. Hueck, N. Luick, L. Mathey, and H. Moritz, Phys. Rev. Lett. **114**, 095301 (2015).
[7] K. W. Madison, F. Chevy, W. Wohlleben, and J. Dalibard, Phys. Rev. Lett. **84**, 806 (2000).
[8] M. Zwierlein, J. Abo-Shaeer, A. Schirotzek, C. Schunck, and W. Ketterle, Nature (London) **435**, 1047 (2005).
[9] L. A. Sidorenkov, M. K. Tey, R. Grimm, Y.-H. Hou, L. Pitaevskii, and S. Stringari, Nature (London) **498**, 78 (2013).
[10] J. Wilks and D. Betts, *An Introduction to Liquid Helium* (Oxford Science Publications, Clarendon Press, Oxford, 1987).
[11] D. Dries, S. E. Pollack, J. M. Hitchcock, and R. G. Hulet, Phys. Rev. A **82**, 033603 (2010).
[12] I. Ferrier-Barbut, M. Delehaye, S. Laurent, A. T. Grier, M. Pierce, B. S. Rem, F. Chevy, and C. Salomon, Science **345**, 1035 (2014).
[13] T. Ozawa, A. Recati, M. Delehaye, F. Chevy, and S. Stringari, Phys. Rev. A **90**, 043608 (2014).
[14] R. Zhang, W. Zhang, H. Zhai, and P. Zhang, Phys. Rev. A **90**, 063614 (2014).
[15] X. Cui, Phys. Rev. A **90**, 041603 (2014).
[16] J. J. Kinnunen and G. M. Bruun, Phys. Rev. A **91**, 041605 (2015).
[17] M. Abad, A. Recati, S. Stringari, and F. Chevy, Eur. Phys. J. D **69**, 126 (2015).
[18] Y. Castin, I. Ferrier-Barbut, and C. Salomon, C.R. Phys. **16**, 241 (2015).
[19] W. Zheng and H. Zhai, Phys. Rev. Lett. **113**, 265304 (2014).
[20] L. Wen and J. Li, Phys. Rev. A **90**, 053621 (2014).
[21] F. Chevy, Phys. Rev. A **91**, 063606 (2015).
[22] H. Shen and W. Zheng, Phys. Rev. A **92**, 033620 (2015).
[23] A. O. Caldeira and A. J. Leggett, Physica (Amsterdam) **121A**, 587 (1983).
[24] C.-H. Chou, T. Yu, and B. L. Hu, Phys. Rev. E **77**, 011112 (2008).
[25] U. Zürcher and P. Talkner, Phys. Rev. A **42**, 3267 (1990).
[26] G. Zürn, T. Lompe, A. N. Wenz, S. Jochim, P. S. Julienne, and J. M. Hutson, Phys. Rev. Lett. **110**, 135301 (2013).
[27] See Supplemental Material at http://link.aps.org/supplemental/10.1103/PhysRevLett.115.265303 for extra comments and discussion.
[28] R. Combescot, M. Y. Kagan, and S. Stringari, Phys. Rev. A **74**, 042717 (2006).
[29] N. Navon, S. Nascimbène, F. Chevy, and C. Salomon, Science **328**, 729 (2010).
[30] G. Astrakharchik, Ph.D thesis, University of Trento, 2004, arXiv:1412.4529.
[31] S. Stringari, Phys. Rev. A **58**, 2385 (1998).
[32] P. Capuzzi, P. Vignolo, F. Federici, and M. P. Tosi, Phys. Rev. A **73**, 021603 (2006).
[33] L. Luo, B. Clancy, J. Joseph, J. Kinast, and J. E. Thomas, Phys. Rev. Lett. **98**, 080402 (2007).
[34] J. Joseph, B. Clancy, L. Luo, J. Kinast, A. Turlapov, and J. E. Thomas, Phys. Rev. Lett. **98**, 170401 (2007).
[35] V. P. Singh, W. Weimer, K. Morgener, J. Siegl, K. Hueck, N. Luick, H. Moritz, and L. Mathey, arXiv:1509.02168.
[36] C. A. Regal, M. Greiner, and D. S. Jin, Phys. Rev. Lett. **92**, 083201 (2004).
[37] W. Kohn, Phys. Rev. **123**, 1242 (1961).
[38] P. P. Orth, D. Roosen, W. Hofstetter, and K. Le Hur, Phys. Rev. B **82**, 144423 (2010).
[39] R. Onofrio and B. Sundaram, Phys. Rev. A **92**, 033422 (2015).